



OPEN *Asterias amurensis* lipids enhance the immunity of immunosuppressed mice as sustainable marine-eco materials

Ju Hyun Nam^{1,8}, JeongUn Choi^{1,2,8}, Weerawan Rod-in^{2,3,4}, A-yeong Jang², Jun Jae Jung⁵, Sang-min Lee⁶ & Woo Jung Park^{1,2,7}✉

Starfish (*Asterias amurensis*) are important predators in the marine benthic environment, preying on mollusks and echinoderms. Their waste also causes significant environmental harm. However, starfish contain a variety of nutrients and biologically active compounds that require further investigation. To maintain marine ecosystems and address environmental waste, lipids were extracted from *A. amurensis* skin, and their immune-enhancing effects were evaluated in cyclophosphamide (CY)-induced immunosuppressive mice. *A. amurensis* lipids were combined with PEG 6000 (AA-PEG), which contains a high content of polyunsaturated fatty acids (PUFAs, 49.44%), primarily C20:5n3. Mice were administered various dosages of AA-PEG, ranging from 50 to 200 mg/kg body weight (BW) via oral delivery and CY injection. Results revealed that AA-PEG at 150 mg/kg BW promoted the recovery of cellular immune function in both splenocytes from the spleen and peritoneal macrophages, similar to the normal group. Administration of AA-PEG (50–150 mg/kg BW) gradually raised the spleen index (2.2–2.5 mg/g) and natural killer (NK) cell activity (91–102%), and enhanced ConA- or LPS-stimulated splenocyte proliferation. Subsets of T-lymphocytes (CD4+ and CD8+) dose-dependently increased by AA-PEG. The phagocytic capacity (58–82%) and proliferation (69–98%) of peritoneal macrophages, which had been reduced by CY, were restored with AA-PEG. AA-PEG boosts immunity by promoting nitric oxide (NO) generation (84–103%). Furthermore, AA-PEG has been shown to increase immune-related cytokines in splenocytes and peritoneal macrophages, indicating a potential enhancement of Th1 and Th2 activity. These results suggest that AA-PEG restored the immune function of immunosuppressed mice and could be used as an effective immunomodulatory agent, which may play a crucial role in maintaining environmental sustainability.

Keywords Lipid, *Asterias amurensis*, Immunosuppression, Cyclophosphamide

Asterias amurensis (starfish) is a marine invertebrate native to the North Pacific Ocean, particularly around Korea, Japan, and Russia. It belongs to the family Asteroidea, class Asterozoa, and phylum Echinodermata. It has been classified as a significant pest and can have a major impact on marine ecosystems when introduced to non-native areas, as it can become an invasive species^{1,2}. When a starfish enters a new ecosystem outside its native range, it can threaten the sustainability of the marine ecosystem because it is a predator in the marine benthic system, preying on shellfish and other native organisms¹. The starfish severely damages the shellfish farming sector and even significantly reduces native biodiversity since it feeds on shellfish including abalone clams, blood shellfish, and scallops³. Their wastes cause significant harm to the environment⁴, which can lead to a reduction in the population of native species and alter the ecological balance⁵. Without control ways, its spread

¹Department of Wellness-Bio Industry, Gangneung-Wonju National University, Gangneung, Gangwon 25457, Republic of Korea. ²Department of Marine Bio Food Science, Gangneung-Wonju National University, Gangneung, Gangwon 25457, Republic of Korea. ³Department of Agricultural Science, Faculty of Agriculture Natural Resources and Environment, Naresuan University, Phitsanulok 65000, Thailand. ⁴Center of Excellence in Research for Agricultural Biotechnology, Naresuan University, Phitsanulok 65000, Thailand. ⁵East Coast Life Sciences Institute, Gangneung-Wonju National University, Gangneung, Gangwon 25457, Republic of Korea. ⁶Department of Aquatic Life Medicine, Gangneung-Wonju National University, Gangneung, Gangwon 25457, Republic of Korea. ⁷KBioRANCh Co., Ltd, Gangneung, Gangwon 25457, Republic of Korea. ⁸Ju Hyun Nam and JeongUn Choi contributed equally. ✉email: pwj0505@gwnu.ac.kr

may result in the loss of sustainability and stability in the marine ecosystem⁶. In order to solve environmental wastes, fishermen preserve a considerable quantity of starfish, which they use as fertilizer and occasionally waste⁷. In Hokkaido, starfish around 15,000 tons are disposed of as expensive industrial waste each year⁸, which has caused to maintain the marine ecosystem. On the other hand, if its population is well-managed, starfish can be part of a sustainable marine ecosystem.

However, starfish have been reported to possess a variety of bioactive compounds, including steroids, steroid glycosides, anthraquinones, alkaloids, polysaccharides, peptides, and fatty acids (FAs)⁹. These compounds exhibit anti-cancer, anti-fungal, anti-inflammatory, and immune-enhancing activities^{4,10–13}. Previous studies have reported that FAs extracted from the skin, gonad, and D-gland of *A. amurensis* contained high amounts of dihomo- γ -linolenic acid (20:3n-6) and eicosapentaenoic acid (EPA), which demonstrated anti-inflammatory and immune-enhancing activities on macrophage cells^{12,13}. Therefore, these functional materials and nutrients can be critical to retain nature sustainability and this study suggested that the lipids extracted from *A. amurensis* skin have immune effects on immunosuppressed mice induced by CY, indicating that the lipids could be considered as an effective immunomodulatory agent.

The immune system is a structure of cells and molecules that have specialized roles in defense against infection and comprises of two fundamentally different types of reactions to invading microorganisms¹⁴. Immune responses such as the immune organ indexes (bone marrow, spleen, thymus) and population change of immune cells (macrophages, splenocytes, neutrophils, NK cells) are essential mechanisms for the enhancement of the body's immune function¹⁴. They can activate a variety of immunomodulatory functions by producing cytokines such as interferon- γ (IFN- γ), tumor necrosis factor- α (TNF- α), interleukin-2 (IL-2), and, IL-6, and other inflammatory mediators^{15,16}. Cyclophosphamide (CY) as a chemotherapy agent, is used to treat cancer, autoimmune and immune-mediated diseases¹⁷. CY-induced immunosuppressive animal models were typically used to determine immunomodulatory effects that have an inhibitory effect on immune functions, such as the reducing indexes of spleen and thymus, as well as the downregulation of some cytokine secretion^{18–20}.

In general, lipids are hydrophobic or amphiphilic small molecules that cannot dissolve in water but can dissolve in nonpolar solvents, such as alcohol, ether, chloroform, and benzene²¹. The bioactive lipid mediators in immune cells are synthesized from lipids, especially fatty acids, which are major components of living organisms^{22,23}. It has been reported that polyunsaturated fatty acids (PUFAs), in particular EPA (20:5n-3), and docosahexaenoic acid (DHA, C22:6n-3) can have anti-tumor, immunomodulatory, and anti-diabetic properties as well as inflammatory diseases and Alzheimer's disease^{12,13,22,24–27}. In addition, PUFAs have been shown to modulate cyclophosphamide-induced immunosuppression in animal models^{28,29}. Previously, Liu et al.³⁰ reported that *A. rollestoni* polysaccharides contained the immune-enhancement effects in macrophages and CY-induced immunosuppression mice. However, the immune-enhancing activity of *A. amurensis* has not been shown *in vivo* mice physiological system. Therefore, the current study evaluated the effect of oral administration of the lipids extracted from *A. amurensis* skin on immunosuppressed mice induced by CY, which showed the functional materials to be crucial to maintain nature sustainability, solving the environmental problems in the marine ecosystem.

Results

Fatty acid compositions form *A. amurensis* lipids combined with PEG 6000 (AA-PEG)

Fatty acid profiles (% of total FA) of experimental diets are shown in Table 1. The main effect of AA-PEG was significant ($p < 0.05$), influencing the levels of several FAs: 15.16% SFAs, 35.40% MUFAs, and 49.44% PUFAs. Among the FAs, EPA (C20:5n3) showed the highest content at 24.07%. Major SFAs included palmitic acid (C16:0, 4.08%), arachidic acid (C20:0, 5.95%), and behenic acid (C22:0, 2.56%). Major MUFAs included oleic acid (C18:1n9, 8.12%), and vaccenic acid (C18:1n7, 2.24%), and palmitic acid (C20:1n7, 22.73%). PUFAs were the most abundant, consisting of EPA, dihomo- γ -linolenic acid (20:3n-6, 17.78%), and DHA (C22:6n3, 5.03%).

Effects of AA-PEG on spleen index

The effects of AA-PEG on the spleen size and spleen index are shown in Fig. 1. The spleen size and spleen index of the CY-treated groups significantly decreased when compared to the normal group (N). The group treated with ginseng (GIN) and levamisole (LEV) increased the spleen index and spleen size compared to the CY group. The spleen size and index of the AA-PEG treatment groups increased to 150 mg/kg BW in a dose-dependent manner, but slightly decreased at 200 mg/kg BW, whereas no significant difference ($p < 0.05$) was found between the PEG 6000 (PEG) and CY groups.

Effects of AA-PEG on peritoneal macrophage proliferation

The effects of various concentrations of AA-PEG on the cell proliferation of peritoneal macrophages are shown in Fig. 2A. Compared to normal group mice, cell proliferation in the CY group decreased. Administration of AA-PEG (50–200 mg/kg BW) significantly increased the macrophage proliferation in a dose-dependent manner up to 150 mg/kg BW, while the macrophage proliferation of AA-PEG at 200 mg/kg BW was lower than AA-PEG at 150 mg/kg BW. In addition, AA-PEG at 150 mg/kg BW restored cell proliferation similar to that of the normal group.

Effects of AA-PEG on NO production

Our results showed that the production of NO in the CY group was remarkably lower than in the normal group (Fig. 2B). After being administrated with AA-PEG, there was a significant recovery in NO production compared with the CY group. The NO production of AA-PEG at 150 mg/kg BW was greater than at other concentrations.

Fatty acids	Total fatty acids (%)
C14:0	0.88 ± 0.10 ^{jk}
C15:0	0.90 ± 0.02 ^{jk}
C16:0	4.08 ± 0.10 ^g
C18:0	0.80 ± 0.03 ^k
C20:0	5.95 ± 0.18 ^e
C22:0	2.56 ± 0.05 ^h
C16:1n7	1.63 ± 0.07 ⁱ
C18:1n9	8.12 ± 0.23 ^d
C18:1n7	2.24 ± 0.10 ^{hi}
C20:1n7	22.73 ± 2.05 ^b
C22:1n9	0.69 ± 0.02 ^k
C18:3n3	0.32 ± 0.02 ^k
C20:2n6	1.56 ± 0.04 ^{ij}
C20:3n3	17.78 ± 0.47 ^c
C20:5n3	24.07 ± 0.60 ^a
C22:5n3	0.68 ± 0.01 ^k
C22:6n3	5.03 ± 0.19 ^f
Totals SFAs	15.16 ± 0.45
Totals MUFAs	35.40 ± 1.73
Totals PUFAs	49.44 ± 1.28

Table 1. Fatty acid compositions (% of total fatty acids) of AA-PEG. Values are presented as means ± SD (*n* = 5). Significant differences (*p* < 0.05) are indicated by different superscript letters in the table.

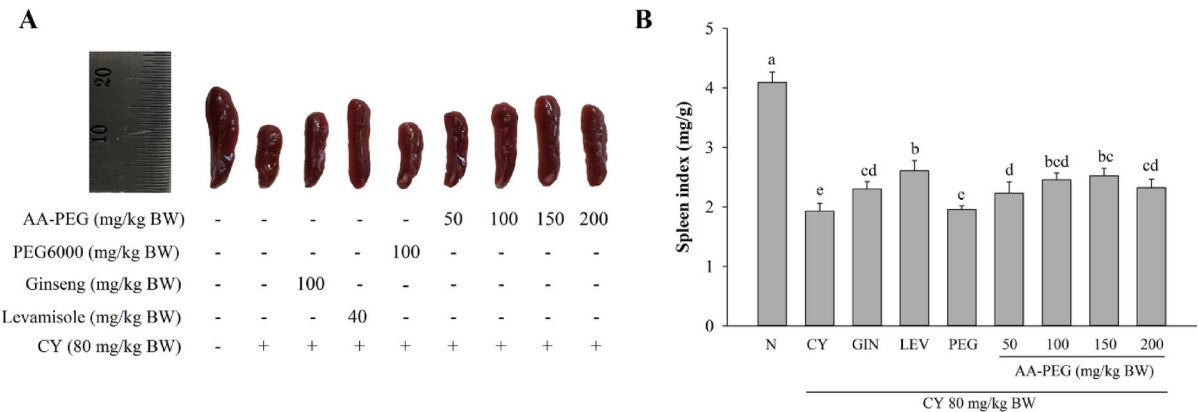


Fig. 1. Effects of AA-PEG on spleen size and spleen index in CY-treated mice. (A) Spleen size effects, (B) Spleen index effects. Results are expressed as means ± SD. Different letters (a-e) indicate significant (*p* < 0.05) differences among all the groups.

Effects of AA-PEG on peritoneal macrophage phagocytosis

The phagocytosis ratio of peritoneal macrophages from normal mice was considered to be 100% by the neutral red uptake method. As shown in Fig. 2C, the CY-treated mice significantly reduced macrophage phagocytosis as compared with the normal group (*p* < 0.05). The phagocytic activities of peritoneal macrophages were improved after treatment with AA-PEG in a dosage-dependent manner (50–150 mg/kg BW), whereas AA-PEG at a dose of 200 mg/kg BW reduced macrophage phagocytosis slightly as compared to AA-PEG at 150 mg/kg BW. Moreover, the phagocytosis of the AA-PEG at 150 mg/kg BW was enhanced to the same level as that of the positive group, which increased by 88.96%.

Effects of AA-PEG on gene expression in peritoneal macrophages

Real-time qPCR was used to analyze the mRNA expression levels of *iNOS*, *COX-2*, *IL-1β*, *IL-6*, and *TNF-α*. As shown in Fig. 3, the expression of these genes was remarkably downregulated in the CY group. In the AA-PEG-treated group, different dosages of AA-PEG can significantly up-regulate the mRNA expression of *iNOS*, *COX-2*, *IL-1β*, *IL-6*, and *TNF-α*, compared with the only CY treated group. Especially, the mRNA levels of *COX-2*, *IL-1β*, *IL-6*, and *TNF-α* at the dose of AA-PEG (150 mg/kg BW) reached a level above the levamisole and ginseng (positive control) groups.

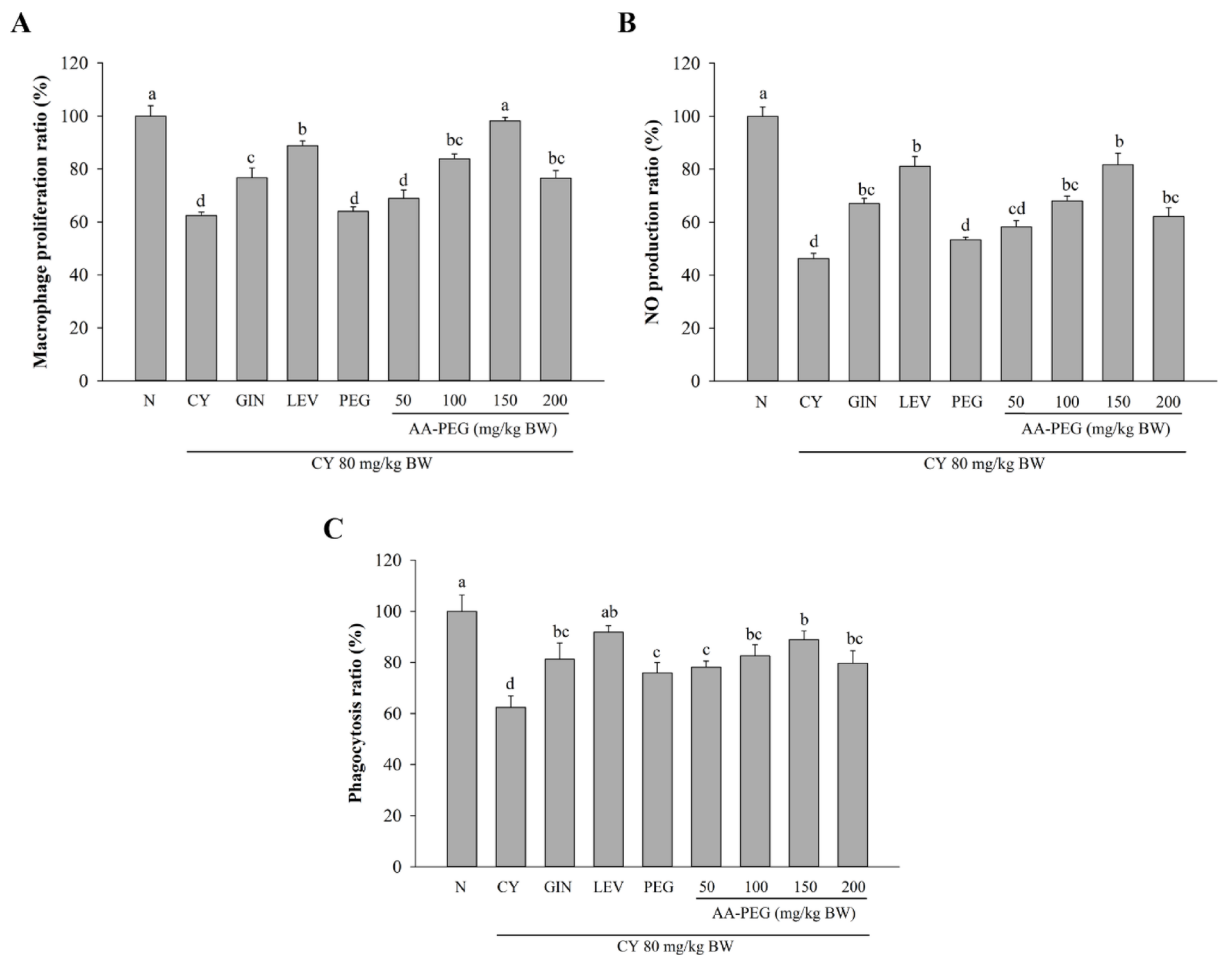


Fig. 2. Effects of AA-PEG on macrophage proliferation, NO production, and phagocytosis activity in peritoneal macrophages in CY-treated mice. **(A)** Influence on macrophage proliferation, **(B)** Influence on NO production, **(C)** Influence on phagocytosis activity. Results are expressed as means \pm SD. Different letters (a–d) indicate significant ($p < 0.05$) differences among all the groups.

Effect of AA-PEG on NK cell activity

The NK cell activity of splenocytes was measured by examining the cytotoxicity of YAC-1 cells. As shown in Fig. 4A, the NK cell activity of the CY group was clearly inhibited compared to that of the normal group. However, the NK cell activity of the groups treated with various doses of AA-PEG was increased, higher than that of the CY group. In particular, the NK cell activity of AA-PEG at a dose of 150 mg/kg BW was restored to a level similar to the normal and levamisole groups.

Effect of AA-PEG on splenocyte proliferation

To evaluate the effects of AA-PEG on mitogen-stimulated splenic lymphocyte proliferation, ConA- and LPS-induced splenocyte proliferation were performed to assess T- and B-lymphocyte proliferation activities^{20,31,32}. As shown in Fig. 4B, the administration of CY significantly reduced T-cell and B-cell proliferation compared with the normal group. However, the splenocyte proliferation of AA-PEG-treated mice was significantly increased in a dose-dependent manner when compared with the CY group. At the dose of 200 mg/kg BW, AA-PEG also significantly increased splenocyte proliferation compared with the CY group, but lower than the doses of 100 and 150 mg/kg BW. In particular, AA-PEG at a dose of 150 mg/kg BW, the splenic lymphocyte proliferation was similar to or higher than that of the positive group.

Effect of AA-PEG on gene expression of splenic lymphocytes

Figure 5 showed the effects on the mRNA expression of immune-associated genes in splenocytes. Compared to the CY group, these genes significantly enhanced the expression levels of AA-PEG at 50–150 mg/kg BW ($p < 0.05$) in a dose-dependent manner. However, AA-PEG at 200 mg/kg BW increased expression levels more than the CY group, but lower than AA-PEG at 100 and 150 mg/kg BW. At a dose of 150 mg/kg BW, the expression levels of cytokines such as *IL-1 β* , *IL-2*, *IL-4*, *IL-6*, *TNF- α* , and *IFN- γ* was recovered similarly to those of the normal group.

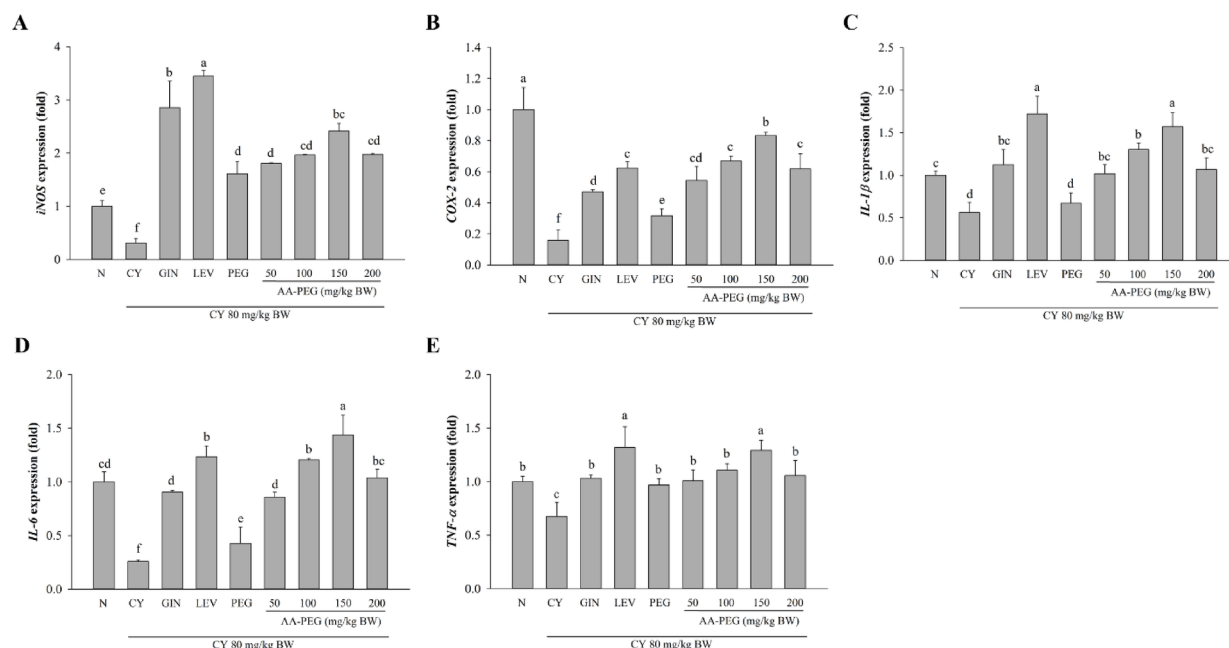


Fig. 3. Effects of AA-PEG on mRNA expression in LPS-stimulated peritoneal macrophages in CY-treated mice. The relative levels of *iNOS* (A), *COX-2* (B), *IL-1β* (C), *IL-6* (D), and *TNF-α* (E) expression. Results are expressed as means ± SD. Different letters (a-f) indicate significant ($p < 0.05$) differences among all the groups.

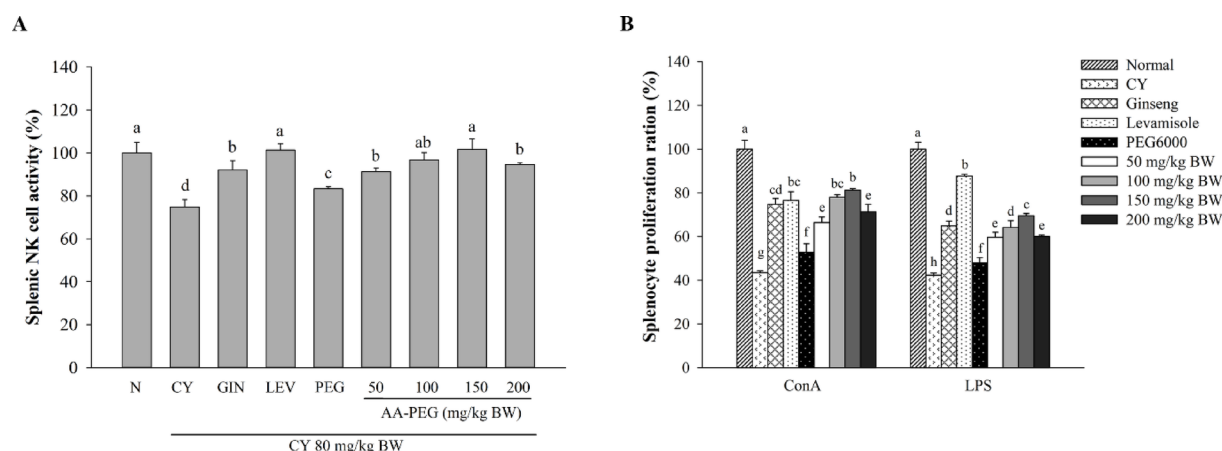


Fig. 4. Effects of AA-PEG on splenic NK cell activity and mitogen-stimulated splenocyte proliferation in CY-treated mice. (A) Effects on NK cell activity in spleen, (B) Effects on splenocyte proliferation. Results are expressed as means ± SD. Different letters (a-g) indicate significant ($p < 0.05$) differences among all the groups.

Effect of AA-PEG on CD4 + and CD8 + lymphocytes

As shown in Fig. 6A and B, the percentages of CD4 + and CD8 + T cells, as well as the CD4+/CD8 + ratio, were significantly lower than in the normal group and higher than in the CY group. Treatment with AA-PEG increased the percentage of helper T cells compared with mice in the CY-treated group. Moreover, AA-PEG upregulated the CD4+/CD8 + ratio in splenocytes at the tested dose (50–200 mg/kg), compared to those in the CY group.

Discussion

Starfish are an invasive species in the marine ecosystem, causing productivity loss and damaging the natural environment due to the rapid increase in their populations³³. However, starfish are still valuable and contain many bioactive compounds, such as saponins, polysaccharides, peptides, amino acids, collagen, and alkaloids². Consequently, the utilization of starfish can support environmental sustainability by controlling their populations, reducing waste, creating valuable products, and promoting the conservation of marine ecosystems.

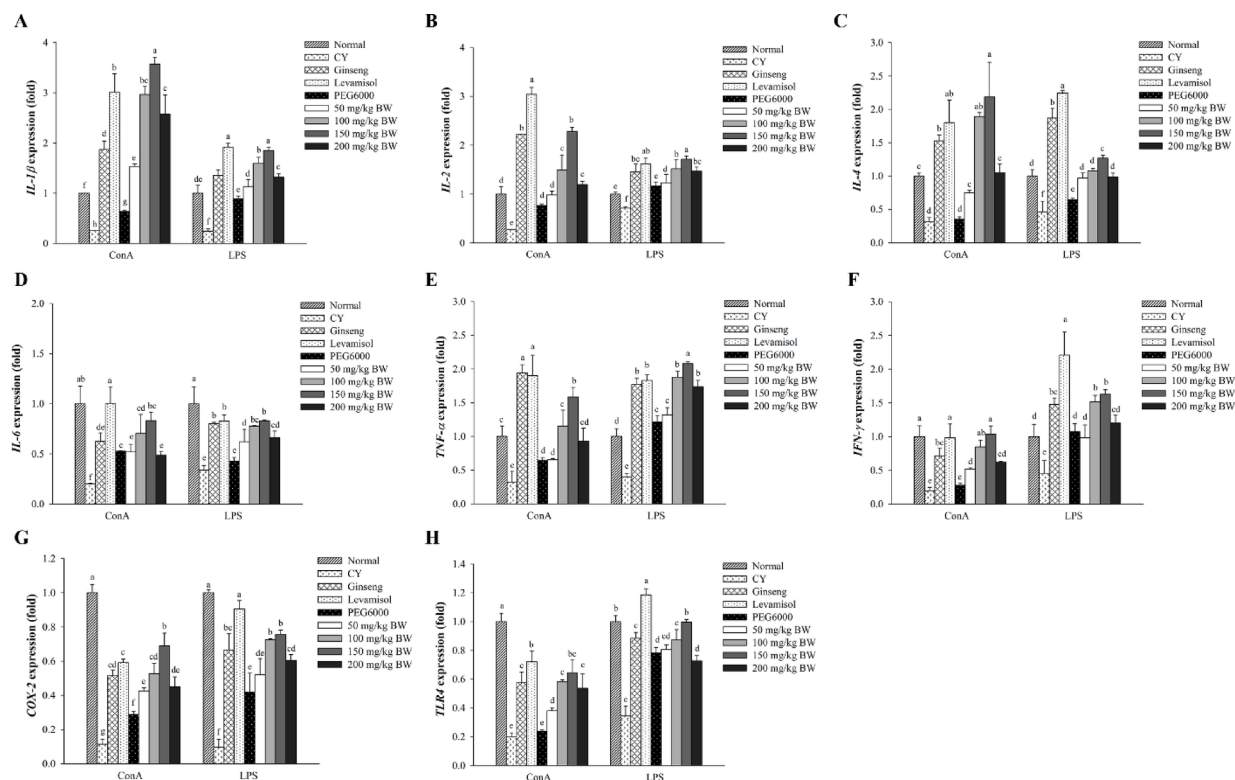


Fig. 5. Effects of AA-PEG on immune-associated gene expression from mitogen-stimulated splenic lymphocyte cells in CY-treated mice. The relative levels of *IL-1 β* (A), *IL-2* (B), *IL-4* (C), *IL-6* (D), *TNF- α* (E), *IFN- γ* (F), *COX-2* (G), and *TLR-4* (H) expression. Results are expressed as means \pm SD. Different letters (a-h) indicate significant ($p < 0.05$) differences among all the groups.

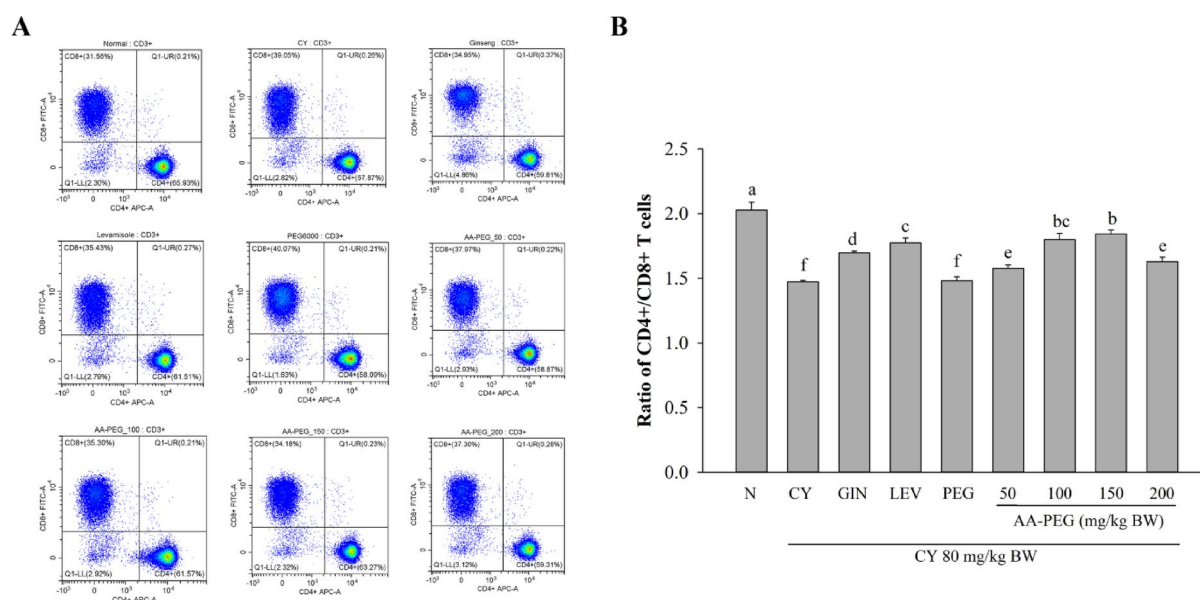


Fig. 6. Effects of AA-PEG on CD4+ and CD8+ T lymphocytes and the ratio of splenic CD4+/CD8+ T cells in CY-treated mice. (A) Effects on CD4+ and CD8+ T lymphocytes, (B) splenic CD4+/CD8+ T cell ratio. Results are expressed as means \pm SD. Different letters (a-f) indicate significant ($p < 0.05$) differences among all the groups.

In our study, we determined the FA contents in AA-PEG. The FAs present in AA-PEG were composed of 15% saturated fats, 35% monounsaturated fats, and a significant amount of polyunsaturated fats (49%). PUFAs, such as α -linolenic acid (ALA; C18:3n-3), EPA, and DHA, are essential fatty acids that the body cannot produce and must be obtained through the diet. According to earlier research, PUFAs have been shown to improve a variety of human health conditions, including cardiovascular disease, inflammation, obesity, cancer, and many others³⁴. Other FAs, such as palmitic acid and oleic acid, are key dietary sources for growth, energy, metabolic synthesis, and components of cell membranes, and they also perform well in eliciting immunological responses^{35,36}. Our findings reveal that the FA profile of EPA had the highest content in AA-PEG, which has immune-enhancing effects on immune cells³⁷.

In this study, the immune-enhancing effects of AA-PEG were established in CY-induced immunosuppressed BALB/c mouse models, and the immunological action of lipids is most likely initiated by the activation of effector immune cells. Therefore, we investigated the effects of AA-PEG on peritoneal macrophages and splenocytes. *In vivo* experiments, several research on the immunomodulatory effects of various materials in a CY-induced immunosuppression animal model have been conducted^{18–20,32}. AA-PEG was obtained from the lipids extracted from *A. amurensis* skin combined with PEG 6000. PEG is widely used in biomedical applications such as bioconjugation³⁸, drug delivery^{38,39}, surface functionalization⁴⁰, and tissue engineering⁴¹. PEG-lipid conjugates are commonly utilized to produce a polymer coat in the field of liposomal drug delivery⁴². In addition, ginseng syrup and levamisole, an immune enhancer, were used as positive controls for comparing the efficacy of AA-PEG.

Macrophages, important effector cells, are phagocytes derived from monocytes of the innate immune system and play a key role in initiating and propagating adaptive immunity⁴³. Activated macrophages can actively perform phagocytosis, which is the first step in the defense against invading pathogens. It refers to the process by which certain body cells, known as phagocytes, ingest and eliminate microbes, malignant cells, and tissue debris⁴⁴. In this study, the proliferative capacity and phagocytosis indices of peritoneal macrophages significantly increased after AA-PEG treatment. In addition, the production of NO by the nitric oxide enzyme (NOS) is harmful to pathogenic bacteria and causes tumor cell death, indicating that macrophages are activated during immunological responses⁴⁵. After the administration of AA-PEG, NO production was found to be elevated in our studies. In addition, AA-PEG also enhanced the cell functions of peritoneal macrophages, including proliferation, phagocytic activity, and NO production, showing results comparable to or better than positive control drugs such as ginseng syrup and levamisole. Thus, these results may explain the immune-modulating effect of AA-PEG on macrophages.

The spleen is one of the immune organs that play important roles in the body's immune function³². Several compounds have also been reported to significantly improve the spleen indices of mice, which are indicators of the development of their immune system^{19,20}. Furthermore, CY treatment usually causes damage and weight loss in the spleen, which acts as a representative immunological organ⁴⁶. Thus, to evaluate the immunostimulatory effect of AA-PEG in a CY-induced immunosuppressive mouse model, we assessed the rise in the weights of these immune organs. After the administration of CY, the immune organ index of mice was significantly decreased. However, after treatment with AA-PEG, the spleen index significantly increased ($p < 0.05$) at 150 mg/kg BW compared to the CY group, consistent with previous studies^{46,47}. These results showed that *A. amurensis* lipids can recover from damage to immune organs caused by CY.

Lymphocytes are the most abundant immune cells in the spleen, and their functional status has a direct impact on immunological activity of the spleen⁴⁸. Splenic lymphocyte proliferation is an important event that reflects both cellular and humoral immune responses. Lymphocytes stimulated by ConA can be used to evaluate T lymphocyte activity related to cellular immunity, and lymphocytes stimulated by LPS can be used to evaluate B lymphocyte activity related to humoral immunity^{14,31}. Thus, to assess the immunostimulatory activity of AA-PEG on lymphocytes, we investigated the ConA- and LPS-induced splenocyte proliferation to evaluate T- and B-lymphocyte proliferation activities. Our results demonstrated that AA-PEG increased the cytotoxicity of NK cells and splenic lymphocyte proliferation up to 150 mg/kg BW, but these effects decreased at the highest concentration (200 mg/kg BW). Likewise, polysaccharide obtained from *Craterellus cornucopioides* at a high dose (240 mg/kg) reduced splenocyte proliferation in the mouse model of CY-induced immunosuppression¹⁶. Another type of splenic lymphocyte, natural killer (NK) cells are cytotoxic lymphocytes with a nonspecific ability to kill abnormal and foreign cells, and are present in the early phases of immune responses^{49,50}. The measurement of NK cell activity is a useful method for evaluating cellular immunity in a host⁵⁰. However, treatment with AA-PEG restored NK cell activity against the CY treatment, which suggests AA-PEG could contribute to the regulation of NK cell activity. The results indicated that AA-PEG promoted peritoneal macrophage phagocytosis as well as the immune effects of NK, T, and B lymphocytes in immunosuppressive mouse models.

In the innate and adaptive immune responses, cytokines are important factors in mediating and regulating the immune response. The T lymphocytes are regulators of adaptive function, serving as primary effectors for cell-mediated immunity⁵¹. They can be divided into two effector cell subsets based on their function and the cytokines they produce. Th1 and Th2 cells secrete various types of cytokines to regulate immunity, leading to different cellular responses. For example, Th1 cells produce IL-2, IFN- γ and TNF- α , while Th2 cells produce cytokines such as IL-4, IL-5, and IL-10³¹. Compared with mice treated with CY, the mixture of anionic macromolecules extracted from *Codium fragile* and red ginseng significantly up-regulated the expression of cytokine, such as IL-1 β , IL-6, TNF- α , IFN- γ , COX-2, iNOS, and TLR-4 genes in peritoneal macrophages⁵². *Echinacea purpurea* extract reversed the CY-induced decrease IL-2, TNF- α and IFN- γ levels in splenic lymphocytes⁵³. In this study, the levels of expression of immune-related genes increased with increasing doses of AA-PEG in splenic lymphocytes and peritoneal macrophages, and the highest level of expression occurred at the 150 mg/kg BW (Figs. 3 and 5). Thus, AA-PEG can markedly promote the mRNA expression of immune-associated genes in the immunosuppressive

mice induced by CY and improve the immune function thought activating peritoneal macrophages, which is consistent with other reports^{16,47}.

T cells are defined by their surface receptor expressions and are comprise several subtypes. CD3 (cluster of differentiation 3) is involved in the activation of both cytotoxic T cells (CD8 + naive T cells) and T helper cells (CD4 + naive T cells), both of which are important regulators of immunological responses⁵¹. CD4 + T-helper lymphocytes recognize exogenous antigens presented in MHC class II molecules, whereas CD8 + T lymphocytes recognize endogenous antigens presented in molecules^{51,54}. In this study, The CD4+/CD8 + ratio of splenic lymphocytes was improved in proportion to the administered dose of AA-PEG, reaching at 150 mg/kg BW (Fig. 6). These results are consistent with previous research^{18,55}, indicating that the proportion of CD4 + and CD8 + T lymphocytes was improved by AA-PEG.

In conclusion, the current study demonstrates the potential of skin starfish lipids as AA-PEG by repurposing marine by-products as a sustainable material with environmental benefits and functional applications in immune modulation. AA-PEG can restore immunosuppression in CY-treated mice through its effects on immune modulation, including peritoneal macrophage proliferation, NO production, macrophage phagocytosis, spleen index, splenic NK cell activity, and splenic lymphocyte proliferation. AA-PEG administration also significantly inhibited immune-regulated gene expression in peritoneal macrophages and splenic lymphocytes. Flow cytometry analysis revealed an increased CD4/CD8 ratio in T-lymphocytes from the spleens of CY-induced mice. Thus, AA-PEG could contribute to advancements in immune-regulation treatments while promoting environmental sustainability.

Materials and methods

Lipid extraction from *Asterias amurensis* skin

Asterias amurensis was collected from the east coast of Gangneung, Gangwon-do, South Korea. The skin of *A. amurensis* was isolated and collected. The samples were dried in the sunlight for at least 3 days. The dried skins were then crushed with a grinder and stored at -20°C until used for lipid extraction.

Lipids were extracted according to a modified Bligh and Dyer method⁵⁶. Briefly, 4.5 g of samples were mixed with chloroform: methanol (1:2, v/v) and homogenized for 2 min. 10 mL of chloroform and distilled water were added and homogenized for 30 s. After that, the mixture was centrifuged at 3000 rpm for 10 min at 4°C . After centrifugation, the organic solvent was filtered with Whatman No.1 filter paper, and through a $0.2\ \mu\text{m}$ PETE membrane. The supernatant was removed and concentrated under a vacuum and nitrogen evaporator. Finally, the dried lipids were dissolved with absolute alcohol.

Combination with lipids from *A. amurensis* and PEG 6000 (AA-PEG)

For use in animal experiments, the extracted lipids were mixed with PEG 6000 in a ratio of 1:1 (w/w) according to the previous report⁵⁷. The lipids were added to PEG 6000 to produce a homogenized mixture at 60°C . The solution was removed in a rotary evaporator under vacuum at 40°C and 45 rpm for 2 h, and then stored at -20°C for 24 h. After breaking the mixture, the samples were mashed through a 100-mesh sieve and stored in a desiccator.

Analyzing the profiles of fatty acids

The fatty acids were extracted from the AA-PEG according to the method of Garces and Mancha^{58,59} to prepare fatty acid methyl esters (FAMES) via a one-step hydrolysis, extraction, and methylation process. The fatty acid profiles were analyzed by gas chromatography with flame ionization detection (GC-FID), which was carried out on a 7890 A (Agilent Technologies, CA, USA), and the GC-FID system was used as previously described⁶⁰.

Animals and immunosuppressive treatments in mice

A total of 45 male BALB/c mice (6 weeks old, body weight 21–23 g) were purchased from the Central Lab, Animal Inc. (Seoul, Korea). The mice were maintained at a constant temperature ($22^{\circ}\text{C} \pm 2^{\circ}\text{C}$) under a 12-h dark-light cycle. A standard laboratory diet and water were provided to all mice. The Institutional Animal Care and Use Committee (IACUC) at Gangneung–Wonju National University in South Korea granted approval for this study (Approval Number: GWNU-2021-12). All animal methods were performed in accordance with the relevant guidelines and regulations. All authors complied with the guidelines for animal research: reporting of in vivo experiments (ARRIVE).

After 1 week of acclimatization, the mice were randomly divided into 9 groups ($n = 5$) for various treatments. For 10 days, healthy mice were treated daily with saline solution by gavage normal controls (Normal group). Other mice were received oral administration daily for 10 days as follows: negative control (CY group) group of mice were received saline solution; LEV group of mice as positive controls were received levamisole (40 mg/kg BW); GIN group of mice as positive controls were received commercial red ginseng syrup (100 mg/kg BW); PEG group of mice as model controls were received PEG 6000 (100 mg/kg BW); AA-PEG groups of mice were received difference doses of AA-PEG (50, 100, 150, and 200 mg/kg BW). According to a previous study³¹, all mice (except for those in the normal group) were intraperitoneally injected with 80 mg/kg BW of CY to cause immunosuppression from Day 4 to Day 6. Levamisole and commercial red ginseng syrup were used as the positive controls, and both solutions were involved in modulating the inflammatory responses as immunomodulatory agents^{15,52,61}. All mice were euthanized using a CO_2 anesthesia system, in compliance with the guidelines set forth by the American Veterinary Medical Association (AVMA), 24 h after the last treatment.

Determination of spleen size and index

After the mice were sacrificed, the size and index of the spleens were measured. The spleen index was determined using the following formula:

$$\text{Spleen index (mg/g)} = \text{Spleen weight (mg)} / \text{Body weight (g)}$$

Peritoneal macrophages and splenocytes preparation

The mouse was intraperitoneally injected with 5 mL of ice-cold PBS supplemented with 3% of fetal bovine serum (Welgene, Korea). The peritoneal macrophages were collected from the peritoneal cavity of the mouse. Cells were resuspended in RPMI-1640 medium, (Gibco Laboratories, USA) supplemented with 10% of fetal bovine serum, and 1% of streptomycin (100 µg/mL)/penicillin (100 IU/mL) (Welgene, Korea). The cell density was adjusted to 1×10^6 cells/mL.

Splenocytes were isolated from the spleens of BALB/c mice. After weighing, the spleens of each mouse were placed in ice-cold PBS for splenocyte isolation. The splenocytes were extracted using RBC Lysis Buffer (eBioscience, USA), according to the manufacturer's instructions. The cells were transferred to RPMI-1640 medium supplemented with 10% of fetal bovine serum, and 1% of streptomycin (100 µg/mL)/penicillin (100 IU/mL). The cell density was adjusted to 2×10^6 cells/mL.

Analysis of peritoneal macrophage proliferation

Peritoneal macrophage cells were cultured in the presence or absence of 1 µg/mL of lipopolysaccharide (LPS) for 24 h. After incubation, the cultured medium was removed, and then the cells were determined by the EZ-Cytox Cell Viability Assay kit (Daeillab service, Korea) to detect the proliferation of macrophages. The WST solution (110 µL) was added to each well and incubated at 37 °C for 1 h. The absorbance at 450 nm was detected on a microplate reader (Bio-Rad, USA).

Determination of nitric oxide (NO) production

To detect the NO levels, the peritoneal macrophage cells were cultured in the presence or absence of LPS (1 µg/mL) for 24 h. The culture supernatants (100 µL) were mixed with Griess reagent (Sigma-Aldrich, USA) and incubated for 10 min in dark conditions. The absorbance at 540 nm was detected on a microplate reader.

Phagocytosis assay of peritoneal macrophages

Phagocytosis of macrophages was measured by the neutral red uptake method as described⁶². Peritoneal macrophage cells were seeded in 96-well plates and stimulated with 6 µg/mL of LPS for 24 h. After incubation, the cells were washed twice with 1×PBS and added to a 0.09% neutral red solution at room temperature for 30 min. Cells were washed 2–3 times with 1×PBS and added 50% ethanol containing 1% glacial acetic acid to each well. The absorbance at 540 nm was detected on a microplate reader.

Splenocyte proliferation assay

Splenic lymphocyte proliferation was measured by the EZ-Cytox Cell Viability Assay Kit (Daeillab Service, Korea). The splenocytes were seeded in 96-well plates and cultured with 5 µg/mL Con A (T cell mitogen), or 10 µg/mL LPS (B cell mitogen) for 48 h. The non-treated cells (cultured only with RPMI) were used as a normal control group. After incubation for 48 h, 25 µL of EZ-Cytox reagent was added to each well and incubated at 37 °C for 1 h. The absorbance at 490 nm was detected on a microplate reader.

Analysis of splenic NK cell activity

Splenic NK cell activity was measured using splenocytes as effector cells and YAC-1 cells as target cells. The splenocytes were cultured with or without YAC-1 cells at a ratio of 50:1. After 24 h of co-culturing, the supernatant was collected after centrifugation at 250×g for 5 min. The CytoTox 96® Non-Radioactive Cytotoxicity Assay Kit (Promega, USA) was used to determine the NK cell activity.

Real-time qPCR analysis

The Tri reagent (Molecular Research Center, Inc., USA) was employed to extract total RNA from the splenic lymphocytes or peritoneal macrophages, and isolated RNA was reverse-transcribed into cDNA using the High-capacity cDNA Reverse Transcription Kit (Applied Biosystems, USA). To amplify the cDNA, the cDNA was subjected to TB Green® Premix Ex Taq™ II (Takara Bio Inc., Japan), on a QuantStudio™ 3 FlexReal-Time PCR System (ThermoFisher Scientific, USA). Amplification conditions were as follows: initial denaturation at 95 °C for 30 min, followed by 40 cycles of 95 °C for 5 s and 60 °C for 34 s. Table 2 shows the sequences of the primers.

Flow cytometry analysis

Anti-CD3e-PE, anti-CD4-APC, and anti-CD8-FITC antibodies were added to splenic cells for 20 min at 4 °C. After incubation, cells were centrifuged, washed with 1×PBS buffer, and then resuspended in FACs buffer (2% FBS and 0.1% sodium azide in 1×PBS buffer). The CytoFLEX Flow Cytometer was used to determine the percentages of T-cells and B-cells subsets.

Statistical analysis

The means ± standard deviation (SD) is used to express all data. Statistical analysis was carried out by IBM SPSS Statistics Version 23 software (IBM SPSS, USA). One-way ANOVA and Duncan's multiple range test were used to analyze the significant differences among the groups.

Gene	Oligonucleotide sequence (5' to 3')	
	Forward primer	Reverse primer
IL-1β	GGGCCTCAAAGGAAAGAATC	TACCAAGTTGGGGAACCTCTGC
IL-2	CCTGAGCAGGATGGAGAATTACA	TCCAGAACATGCCGAGAG
IL-4	ACAGGAGAAGGGACGCCAT	GAAGCCCTACAGACGAGCTCA
IL-6	AGTTGCCTTCTTGGGACTGA	CAGAATTGCCATTGCACAAC
IFN-γ	CTCAAGTGGCATAGATGT	GAGATAATCTGGCTCTGCAGGATT
TNF-α	ATGAGCACAGAAAGCATGATC	TACAGGCTTGTCACTCGAATT
TLR-4	CGCTCTGGCATCATCTTCAT	GTTGCCGTTTCTTGTCTTCC
COX-2	AGAAGGAAATGGCTGCAGAA	GCTCGGCTTCCAGTATTGAG
iNOS	TTCCAGAATCCCTGGACAAG	TGGTCAAACCTCTGGGGTTC
β-actin	CCACAGCTGAGAGGAAATC	AAGGAAGGCTGGAAAAGAGC

Table 2. Real-time qPCR primer sequences.

Data availability

All data generated or analyzed during this study are included in this published article.

Received: 20 December 2024; Accepted: 25 April 2025

Published online: 16 May 2025

References

1. Wang, Q., Liu, Y., Peng, Z., Chen, L. & Li, B. Genetic diversity and population structure of the sea star *Asterias amurensis* in the Northern Coast of China. *J. Oceanol. Limnol.* **41**, 1593–1601. <https://doi.org/10.1007/s00343-022-1436-3> (2023).

2. Li, L., Yu, Y., Wu, W. & Wang, P. Extraction, characterization and osteogenic activity of a type I collagen from starfish (*Asterias amurensis*). *Mar. Drugs*. **21**, 274. <https://doi.org/10.3390/md21050274> (2023).

3. Hwang, I. H. et al. Complete NMR assignments of degraded Asteroaponins from *Asterias amurensis*. *Arch. Pharm. Res.* **37**, 1252–1263. <https://doi.org/10.1007/s12272-014-0374-9> (2014).

4. Sharmin, F., Ishizaki, S. & Nagashima, Y. Molecular identification, micronutrient content, antifungal and hemolytic activity of starfish *Asterias amurensis* collected from Kobe Coast, Japan. *Afr. J. Biotechnol.* **16**, 163–170. <https://doi.org/10.5897/AJB2016.15776> (2017).

5. Mulinge, J. Effects of environmental change on species diversity. *Int. J. Biol. Macromol.* **3**, 43–53. <https://doi.org/10.47604/ijb.2014> (2023).

6. Doney, S. C. et al. Climate change impacts on marine ecosystems. *Annual Rev. Mar. Sci.* **4**, 11–37. <https://doi.org/10.1146/annurev-v-marine-041911-111611> (2012).

7. Choi, H. S. Study of eco-physiological pepper responses to starfish-based organic soil amendments in open-field and greenhouse cultivations. *Horticulturae* **7** <https://doi.org/10.3390/horticulturae7100344> (2021).

8. Mikami, D., Sakai, S., Sasaki, S. & Igarashi, Y. Effects of *Asterias amurensis*-derived sphingoid bases on the *de Novo* ceramide synthesis in cultured normal human epidermal keratinocytes. *J. Oleo Sci.* **65**, 671–680. <https://doi.org/10.5650/jos.ess16051> (2016).

9. Dong, G. et al. Chemical constituents and bioactivities of starfish. *Chem. Biodivers.* **8**, 740–791. <https://doi.org/10.1002/cbdv.200900344> (2011).

10. Thao, N. P. et al. Steroidal constituents from the starfish *Astropecten polyacanthus* and their anticancer effects. *Chem. Pharm. Bull.* **61**, 1044–1051. <https://doi.org/10.1248/cpb.c13-00490> (2013).

11. Thao, N. P. et al. Anti-inflammatory Asteroaponins from the starfish *Astropecten monacanthus*. *J. Nat. Prod.* **76**, 1764–1770. <https://doi.org/10.1021/np400492a> (2013).

12. Monmai, C. et al. Anti-inflammatory effect of *Asterias amurensis* fatty acids through NF-κB and MAPK pathways against LPS-stimulated RAW264.7 cells. *J. Microbiol. Biotechnol.* **28**, 1635–1644. <https://doi.org/10.4014/jmb.1802.03044> (2018).

13. Monmai, C. et al. Immune enhancement effect of *Asterias amurensis* fatty acids through NF-κB and MAPK pathways on RAW264.7 cells. *J. Microbiol. Biotechnol.* **28**, 349–356. <https://doi.org/10.4014/jmb.1709.09005> (2018).

14. Zhang, W. N. et al. Immunoenhancement effect of crude polysaccharides of *Helvella Leucopus* on cyclophosphamide-induced immunosuppressive mice. *J. Funct. Foods*. **69**, 103942. <https://doi.org/10.1016/j.jff.2020.103942> (2020).

15. Huang, L. et al. *Mesona chinensis* Benth polysaccharides protect against oxidative stress and immunosuppression in cyclophosphamide-treated mice via MAPKs signal transduction pathways. *Int. J. Biol. Macromol.* **152**, 766–774. <https://doi.org/10.1016/j.ijbiomac.2020.02.318> (2020).

16. Guo, M. Z., Meng, M., Feng, C. C., Wang, X. & Wang, C. L. A novel polysaccharide obtained from *Craterellus cornucopioides* enhances Immunomodulatory activity in immunosuppressive mice models via regulation of the TLR4-NF-κB pathway. *Food Funct.* **10**, 4792–4801. <https://doi.org/10.1039/C9FO00201D> (2019).

17. Ahlmann, M. & Hempel, G. The effect of cyclophosphamide on the immune system: implications for clinical cancer therapy. *Cancer Chemother. Pharmacol.* **78**, 661–671. <https://doi.org/10.1007/s00280-016-3152-1> (2016).

18. Zhou, X. et al. Immunomodulatory activity of a novel polysaccharide from *Lonicera japonica* in immunosuppressed mice induced by cyclophosphamide. *PLoS One*. **13**, e0204152. <https://doi.org/10.1371/journal.pone.0204152> (2018).

19. Wang, H. et al. Glycosaminoglycan from *Apostichopus japonicus* induces Immunomodulatory activity in cyclophosphamide-treated mice and in macrophages. *Int. J. Biol. Macromol.* **130**, 229–237. <https://doi.org/10.1016/j.ijbiomac.2019.02.093> (2019).

20. Han, L. et al. Immunomodulatory activity of a water-soluble polysaccharide obtained from Highland barley on immunosuppressive mice models. *Food Funct.* **10**, 304–314. <https://doi.org/10.1039/C8FO01991F> (2019).

21. Zhang, C. et al. Lipid metabolism in inflammation-related diseases. *Analyst* **143**, 4526–4536. <https://doi.org/10.1039/C8AN01046C> (2018).

22. Banskota, A. H. et al. Polar lipids from the marine macroalgae *Palmaria palmata* inhibit lipopolysaccharide-induced nitric oxide production in RAW264.7 macrophage cells. *Phytochemistry* **101**, 101–108. <https://doi.org/10.1016/j.phytochem.2014.02.004> (2014).

23. Fenton, J. I., Hord, N. G., Ghosh, S. & Gurtzell, E. A. Immunomodulation by dietary long chain omega-3 fatty acids and the potential for adverse health outcomes. *Prostaglandins, Leukot. Essent. Fatty Acids*. **89**, 379–390. <https://doi.org/10.1016/j.plefa.2013.09.011> (2013).
24. Yan, L. et al. Omega-3 polyunsaturated fatty acids promote brain-to-blood clearance of β -Amyloid in a mouse model with Alzheimer's disease. *Brain Behav. Immun.* **85**, 35–45. <https://doi.org/10.1016/j.bbi.2019.05.033> (2020).
25. Eraky, S. M., Abdel-Rahman, N. & Eissa, L. A. Modulating effects of omega-3 fatty acids and Pioglitazone combination on insulin resistance through toll-like receptor 4 in type 2 diabetes mellitus. *Prostaglandins Leukot. Essent. Fat. Acids*. **136**, 123–129. <https://doi.org/10.1016/j.plefa.2017.06.009> (2018).
26. Eltweri, A. M. et al. Potential applications of fish oils rich in omega-3 polyunsaturated fatty acids in the management of Gastrointestinal cancer. *Clin. Nutr.* **36**, 65–78. <https://doi.org/10.1016/j.clnu.2016.01.007> (2017).
27. Yates, C. M., Calder, P. C. & Ed Rainger, G. Pharmacology and therapeutics of omega-3 polyunsaturated fatty acids in chronic inflammatory disease. *Pharmacol. Ther.* **141**, 272–282. <https://doi.org/10.1016/j.pharmthera.2013.10.010> (2014).
28. Lee, S. I. & Kang, K. S. Omega-3 fatty acids modulate cyclophosphamide induced markers of immunosuppression and oxidative stress in pigs. *Sci. Rep.* **9**, 2684. <https://doi.org/10.1038/s41598-019-39458-x> (2019).
29. Choi, J., Rod-in, W., Jang, A. & Park, W. J. *Arctoscopy japonicus* lipids enhance immunity of mice with cyclophosphamide-induced immunosuppression. *Foods* **12**, (2023). <https://doi.org/10.3390/foods12173292>
30. Liu, Y., Wu, X., Wang, Y., Jin, W. & Guo, Y. The immunoenhancement effects of starfish *Asterias rollestoni* polysaccharides in macrophages and cyclophosphamide-induced immunosuppression mouse models. *Food Funct.* **11**, 10700–10708. <https://doi.org/10.1039/D0FO01488E> (2020).
31. Kim, J. E. et al. Immune enhancement effects of *Codium fragile* anionic macromolecules combined with red ginseng extract in immune-suppressed mice. *J. Microbiol. Biotechnol.* **29**, 1361–1368. <https://doi.org/10.4014/jmb.1905.05017> (2019).
32. Cho, C. W. et al. *Cheonggukjang* polysaccharides enhance immune activities and prevent cyclophosphamide-induced immunosuppression. *Int. J. Biol. Macromol.* **72**, 519–525. <https://doi.org/10.1016/j.ijbiomac.2014.09.010> (2015).
33. Kim, Y., Jung, S., Park, Y. K., Moon, D. H. & Kwon, E. E. Exploiting starfish in pyrolysis for the enhanced generation of Syngas and CO₂-looping agent. *J. Clean. Prod.* **276**, 123228. <https://doi.org/10.1016/j.jclepro.2020.123228> (2020).
34. Kapoor, B., Kapoor, D., Gautam, S., Singh, R. & Bhardwaj, S. Dietary polyunsaturated fatty acids (PUFAs): uses and potential health benefits. *Curr. Nutr. Rep.* **10**, 232–242. <https://doi.org/10.1007/s13668-021-00363-3> (2021).
35. Zhao, Z. et al. Palmitic acid exerts anti-tumorigenic activities by modulating cellular stress and lipid droplet formation in endometrial cancer. *Biomolecules* **14**, 601. <https://doi.org/10.3390/biom14050601> (2024).
36. Radzikowska, U. et al. The influence of dietary fatty acids on immune responses. *Nutrients* **11**, 2990. <https://doi.org/10.3390/nu11122990> (2019).
37. Gutiérrez, S., Svahn, S. L. & Johansson, M. E. Effects of omega-3 fatty acids on immune cells. *Int. J. Mol. Sci.* **20** <https://doi.org/10.3390/ijms20205028> (2019).
38. Hoang Thi, T. T. et al. The importance of poly(ethylene glycol) alternatives for overcoming PEG immunogenicity in drug delivery and bioconjugation. *Polymers* **12** (298). <https://doi.org/10.3390/polym12020298> (2020).
39. Parveen, S. & Sahoo, S. K. Long Circulating Chitosan/PEG blended PLGA nanoparticle for tumor drug delivery. *Eur. J. Pharmacol.* **670**, 372–383. <https://doi.org/10.1016/j.ejphar.2011.09.023> (2011).
40. Manson, J., Kumar, D., Meenan, B. J. & Dixon, D. Erratum to: polyethylene glycol functionalized gold nanoparticles: the influence of capping density on stability in various media. *Gold. Bull.* **44**, 195. <https://doi.org/10.1007/s13404-011-0023-8> (2011).
41. Shi, R. Polyethylene glycol repairs membrane damage and enhances functional recovery: a tissue engineering approach to spinal cord injury. *Neurosci. Bull.* **29**, 460–466. <https://doi.org/10.1007/s12264-013-1364-5> (2013).
42. Song, L. Y. et al. Characterization of the inhibitory effect of PEG-lipid conjugates on the intracellular delivery of plasmid and antisense DNA mediated by cationic lipid liposomes. *Biochim. Biophys. Acta Biomembr.* **1558**, 1–13. [https://doi.org/10.1016/S0005-2736\(01\)00399-6](https://doi.org/10.1016/S0005-2736(01)00399-6) (2002).
43. D Barbosa, J. et al. In vitro immunostimulating activity of sulfated polysaccharides from *Caulerpa cupressoides* Var. *Flabellata*. *Mar. Drugs*. **17** <https://doi.org/10.3390/md17020105> (2019).
44. Maeda, R., Ida, T., Ihara, H. & Sakamoto, T. Immunostimulatory activity of polysaccharides isolated from *Caulerpa lentillifera* on macrophage cells. *Biosci. Biotechnol. Biochem.* **76**, 501–505. <https://doi.org/10.1271/bbb.110813> (2012).
45. Zha, X. Q. et al. Structural identification and immunostimulating activity of a *Laminaria Japonica* polysaccharide. *Int. J. Biol. Macromol.* **78**, 429–438. <https://doi.org/10.1016/j.ijbiomac.2015.04.047> (2015).
46. Tang, Y. et al. Effects of fucoidan isolated from *Laminaria Japonica* on immune response and gut microbiota in cyclophosphamide-treated mice. *Front. Immunol.* **13** <https://doi.org/10.3389/fimmu.2022.916618> (2022).
47. Chen, X. et al. A polysaccharide from *Sargassum fusiforme* protects against immunosuppression in cyclophosphamide-treated mice. *Carbohydr. Polym.* **90**, 1114–1119. <https://doi.org/10.1016/j.carbpol.2012.06.052> (2012).
48. Lewis, S. M., Williams, A. & Eisenbarth, S. C. Structure and function of the immune system in the spleen. *Sci. Immunol.* **4**, eaau6085. <https://doi.org/10.1126/sciimmunol.aau6085> (2019).
49. Song, Y. R. et al. Enzyme-assisted extraction, chemical characteristics, and immunostimulatory activity of polysaccharides from Korean ginseng (*Panax ginseng* Meyer). *Int. J. Biol. Macromol.* **116**, 1089–1097. <https://doi.org/10.1016/j.ijbiomac.2018.05.132> (2018).
50. Shin, J. S. et al. Immunostimulatory effects of cordycepin-enriched WIB-801CE from *Cordyceps militaris* in splenocytes and cyclophosphamide-induced immunosuppressed mice. *Phytother. Res.* **32**, 132–139. <https://doi.org/10.1002/ptr.5960> (2018).
51. Actor, J. K. in *Introductory Immunology*. 42–58 (eds Actor, J. K.) (Academic, 2014).
52. Kim, J. E. et al. Co-immunomodulatory activities of anionic macromolecules extracted from *Codium fragile* with red ginseng extract on peritoneal macrophage of immune-suppressed mice. *J. Microbiol. Biotechnol.* **30**, 352–358. <https://doi.org/10.4014/jmb.1909.09062> (2020).
53. Kim, H. R. et al. *Echinacea purpurea* alleviates cyclophosphamide-induced immunosuppression in mice. *Appl. Sci.* **12**, 105. <https://doi.org/10.3390/app12010105> (2022).
54. Haabeth, O. A. W. et al. How do CD4+ T cells detect and eliminate tumor cells that either lack or express MHC class II molecules? *Front. Immunol.* **5**, 174. <https://doi.org/10.3389/fimmu.2014.00174> (2014).
55. Jang, M. et al. Immune-enhancing effects of a high molecular weight fraction of *Cynanchum wilfordii* Hemsley in macrophages and immunosuppressed mice. *Nutrients* **8**, 600. <https://doi.org/10.3390/nu8100600> (2016).
56. Bligh, E. G. & Dyer, W. J. A rapid method of total lipid extraction and purification. *Can. J. Biochem. Physiol.* **37**, 911–917. <https://doi.org/10.1139/o59-099> (1959).
57. Wang, J. et al. Preparation, characterization and *in vitro* and *in vivo* evaluation of a solid dispersion of naringin. *Drug Dev. Ind. Pharm.* **44**, 1725–1732. <https://doi.org/10.1080/03639045.2018.1483390> (2018).
58. Garces, R. & Mancha, M. One-step lipid extraction and fatty acid Methyl esters Preparation from fresh plant tissues. *Anal. Biochem.* **211**, 139–143. <https://doi.org/10.1006/abio.1993.1244> (1993).
59. Park, W. J., Kothapalli, K. S. D., Lawrence, P., Tyburczy, C. & Brenna, J. T. An alternate pathway to long-chain polyunsaturates: the FADS2 gene product Delta8-desaturates 20:2n-6 and 20:3n-3. *J. Lipid Res.* **50**, 1195–1202. <https://doi.org/10.1194/jlr.M800630-JL.R200> (2009).

60. Choi, G. S., Lim, J. H., Rod-In, W., Jung, S. K. & Park, W. J. Anti-inflammatory properties of neutral lipids, glycolipids, and phospholipids isolated from *Ammodytes personatus* eggs in LPS-stimulated RAW264.7 cells. *Fish Shellfish Immunol.* **131**, 1109–1117. <https://doi.org/10.1016/j.fsi.2022.10.039> (2022).
61. Chen, L. X. et al. A comparative study on the effects of different parts of *Panax ginseng* on the immune activity of cyclophosphamide-induced immunosuppressed mice. *Molecules* **24**, 1096. <https://doi.org/10.3390/molecules24061096> (2019).
62. Weeks, B. A., Keisler, A. S., Myrvik, Q. N. & Warinner, J. E. Differential uptake of neutral red by macrophages from three species of estuarine fish. *Dev. Comp. Immunol.* **11**, 117–124. [https://doi.org/10.1016/0145-305X\(87\)90013-9](https://doi.org/10.1016/0145-305X(87)90013-9) (1987).

Author contributions

J.H.N. performed the experiments, analyzed the data, and wrote the manuscript. J.C., W.R., and A.J. performed the experiments. W.R. edited the manuscript. W.J.P. designed the experiment, analyzed the data, and wrote the manuscript. The authors that contributed to this research study are as follows: “conceptualization, W.J.P.; methodology, J.H.N., J.C., W.R. and A.J.; software, J.H.N. and W.R.; validation, J.H.N., J.C., and W.R.; formal analysis, J.H.N., J.C., and W.R.; investigation, J.H.N., and J.C., resources, W.J.P.; data curation, W.R. and W.J.P.; writing—original draft preparation, J.H.N.; writing—review and editing, W.R., J.J.J., S.L. and W.J.P.; visualization, J.H.N., J.C., and W.R.; supervision, W.J.P.; project administration, W.J.P.; funding acquisition, W.J.P.

Funding

This research was supported by a grant (RS-2023-00248832) of the Basic Science Research Program through the National Research Foundation (NRF), funded by the Ministry of Education, Republic of Korea. This research was also supported by the Korea Institute of Marine Science & Technology Promotion (KIMST), funded by the Ministry of Oceans and Fisheries (20220042, Korea Sea Grant Program: Gangwon Sea Grant), and the University Emphasis Research Institute Support Program (No. 2018R1 A61 A03023584), funded by the National Research Foundation, Republic of Korea. Additionally, this work was supported by the Technology development Program (RS-2023-00218659) funded by the Ministry of SMEs and Startups (MSS, Korea).

Declarations

Competing interests

The authors declare no competing interests.

Additional information

Correspondence and requests for materials should be addressed to W.J.P.

Reprints and permissions information is available at www.nature.com/reprints.

Publisher's note Springer Nature remains neutral with regard to jurisdictional claims in published maps and institutional affiliations.

Open Access This article is licensed under a Creative Commons Attribution-NonCommercial-NoDerivatives 4.0 International License, which permits any non-commercial use, sharing, distribution and reproduction in any medium or format, as long as you give appropriate credit to the original author(s) and the source, provide a link to the Creative Commons licence, and indicate if you modified the licensed material. You do not have permission under this licence to share adapted material derived from this article or parts of it. The images or other third party material in this article are included in the article's Creative Commons licence, unless indicated otherwise in a credit line to the material. If material is not included in the article's Creative Commons licence and your intended use is not permitted by statutory regulation or exceeds the permitted use, you will need to obtain permission directly from the copyright holder. To view a copy of this licence, visit <http://creativecommons.org/licenses/by-nc-nd/4.0/>.

© The Author(s) 2025